

RESEARCH

Open Access



# Similarity of immune-associated markers in COVID-19 and Kawasaki disease: analyses from bioinformatics and machine learning

Wang Li<sup>1</sup>, Wenjie Zhu<sup>1</sup>, Xiangting Tang<sup>1</sup>, Zhiting Peng<sup>1</sup>, Jiaqi Ye<sup>1</sup> and Shuping Nie<sup>1\*</sup>

## Abstract

**Background** Infection by the SARS-CoV-2 virus can cause coronavirus disease 2019 (COVID-19) and can also exacerbate the symptoms of Kawasaki disease (KD), an acute vasculitis that mostly affects children. This study used bioinformatics and machine learning to examine similarities in the molecular pathogenesis of COVID-19 and KD.

**Methods** We first identified disease-associated modules in KD using weighted gene co-expression network analysis. Then, we determined shared differentially expressed genes (DEGs) in training datasets for KD (GSE100154) and COVID-19 (GSE225220), performed functional annotation of these shared DEGs, and used Cytoscape plug-ins (MCODE and Cytohubba) to characterize the protein-protein interaction (PPI) network and identify the hub genes. We performed Least Absolute Shrinkage and Selection Operator (LASSO) regression and receiver operating characteristic (ROC) curve analysis to identify the most robust markers, validated these results by analysis of two other datasets (GSE73461 and GSE18606), and then calculated the correlations of these key genes with immune cells.

**Results** This analysis identified 26 shared DEGs in COVID-19 and KD. The results from functional annotation showed that the shared DEGs primarily functioned in immune responses, the formation of neutrophil extracellular traps, and NOD-like receptor signaling pathways. There were three key genes (*PGLYRP1*, *DEFA4*, *RETN*), and they had positive correlations with monocytes, M0 macrophages, and dendritic cells, which function as immune infiltrating cells in KD.

**Conclusion** The potential immune-associated biomarkers (*PGLYRP1*, *DEFA4*, *RETN*) along with their shared pathways, hold promise for advancing investigations into the underlying pathogenesis of KD and COVID-19.

**Keywords** COVID-19, Kawasaki disease (KD), Bioinformatics analysis, Immune cell infiltration, Weighted gene co-expression network analysis (WGCNA)

\*Correspondence:

Shuping Nie  
nieping2@126.com

<sup>1</sup>Department of Clinical laboratory, The Eighth Affiliated Hospital, Sun Yat-sen University, 3025 Shennan Middle Road, Shenzhen, Guangdong 518000, China



© The Author(s) 2025. **Open Access** This article is licensed under a Creative Commons Attribution-NonCommercial-NoDerivatives 4.0 International License, which permits any non-commercial use, sharing, distribution and reproduction in any medium or format, as long as you give appropriate credit to the original author(s) and the source, provide a link to the Creative Commons licence, and indicate if you modified the licensed material. You do not have permission under this licence to share adapted material derived from this article or parts of it. The images or other third party material in this article are included in the article's Creative Commons licence, unless indicated otherwise in a credit line to the material. If material is not included in the article's Creative Commons licence and your intended use is not permitted by statutory regulation or exceeds the permitted use, you will need to obtain permission directly from the copyright holder. To view a copy of this licence, visit <http://creativecommons.org/licenses/by-nc-nd/4.0/>.

## Introduction

Kawasaki disease (KD) is a self-limited systemic vascular disease that typically has a sudden onset and primarily affects children under 5 years of age. KD can lead to coronary artery lesions (CALs) if diagnosis and intervention are not prompt [1]. The diagnosis of KD is based on the presence of a combination of symptoms, and there is no single biomarker. The main symptoms are fever (above 39 °C to 40 °C), rash, inflammation of the extremities and mouth, conjunctivitis, and cervical lymphadenopathy. The American Heart Association (AHA) formulated diagnostic criteria for KD in 2004 and revised these criteria in 2017 [2, 3]. These criteria have widespread acceptance in Japan (where KD was first reported) and elsewhere.

Previous studies have reported the presence of KD throughout the world and in children from diverse ethnic backgrounds, and that the highest incidence is in young males from Asia [4–8]. A recent study [9] of KD in children who were younger than 5 years-old reported an annual incidence rate of 371 cases per 100,000 immediately prior to the COVID-19 pandemic (2019) and a substantially lower rate during the pandemic (2020). This reduction may have been due to the implementation of measures designed to prevent the transmission of SARS-CoV-2. Recent studies in China reported the annual incidence rate in children under 4-years-old was more than 100 cases per 100,000 [10, 11]. Other research identified KD as the predominant etiology of acquired heart disease in pediatric patients, exceeding that of rheumatic fever [12]. KD also has important consequences for the development of coronary artery damage in adults [13]. Although much remains unknown about the pathogenesis of KD, some research suggests that one or more specific infectious agents triggers an excessive immune response that manifests as KD in individuals who are genetically susceptible [14].

KD is associated with respiratory virus infection, but no specific pathogen has been found [15]. COVID-19 is a contagious respiratory disease caused by the SARS-CoV-2 virus [16, 17] that rapidly escalated into a global pandemic. Some studies reported an association between COVID-19 and vasculitis, which may occur as a manifestation of a post-viral immunological response [18]. Since the outbreak of the COVID-19 epidemic, the number of reported patients with KD has increased by 30-fold [19], although some of these diagnoses were later reclassified as complications of COVID-19 [20, 21]. Subsequent research also demonstrated a significant association between COVID-19 and KD, in that children with a genetic predisposition may experience a recurrence of KD following infection by SARS-CoV-2 [22]. Importantly, the co-infection of a patient with KD by SARS-CoV-2 and another pathogen could impact the choice of

the initial pharmacotherapy to be used for treatment of KD [23]. However, available evidence is currently insufficient to establish a causal relationship between COVID-19 and KD, and no genetic studies to date support this relationship.

The purpose of the present study was to use a combination of bioinformatics strategies and machine learning techniques to identify genes that function in immunomodulation and potentially affect the pathogenesis of both COVID-19 and KD. Based on it, we aimed to discover some immune-related markers that could provide aid in the identification and treatment of patients with KD. The workflow of our study is depicted in Fig. 1.

## Materials and methods

### Datasets

“Kawasaki disease” and “COVID-19” were used as search terms respectively to screen the relevant data sets in the Gene Expression Omnibus (GEO) (<https://www.ncbi.nlm.nih.gov/geo/>) database. The organism was set as ‘Homo sapiens’. Case and healthy whole blood samples from children were required. After reading the original design, we selected the datasets that conforms to the principle of randomized control and does not violate the ethical standards. Four gene expression datasets were ultimately analyzed (Table 1). GSE100154 (44 samples) had data from 21 patients with KD and 23 healthy controls. GSE73461 (459 samples) had data from 78 patients with KD and 55 healthy controls, in addition to other patients with various infectious diseases. GSE225220 (217 samples) had data from 37 patients with acute COVID-19 and 26 healthy controls, in addition to other patients with multisystem inflammatory syndrome. GSE18606 (48 samples) had data from 20 patients with KD (8 who were not responsive to intravenous immunoglobulin [IVIG] and 12 who were responsive to IVIG) and nine healthy controls; the analysis only included data from 11 of the 12 responsive patients because post-treatment data were missing for one patient.

### Weighted gene co-expression network analysis

Weighted gene co-expression network analysis (WGCNA) was used to explore the relationship between gene co-expression network and clinical phenotype by searching for co-expression gene modules. Modules with similar expression patterns were established using the R(version 4.3.1)package ‘WGCNA’ version 1.72.1 [24]. First, the top 5000 statistically significant genes were selected for subsequent analysis by calculating the median absolute deviation after refining the datasets. Second, the outlier samples significantly deviated from the majority in dataset were eliminated through the ‘hclust’ function after executing cluster analysis. Third, the ‘pickSoftThreshold’ function was employed to determine the

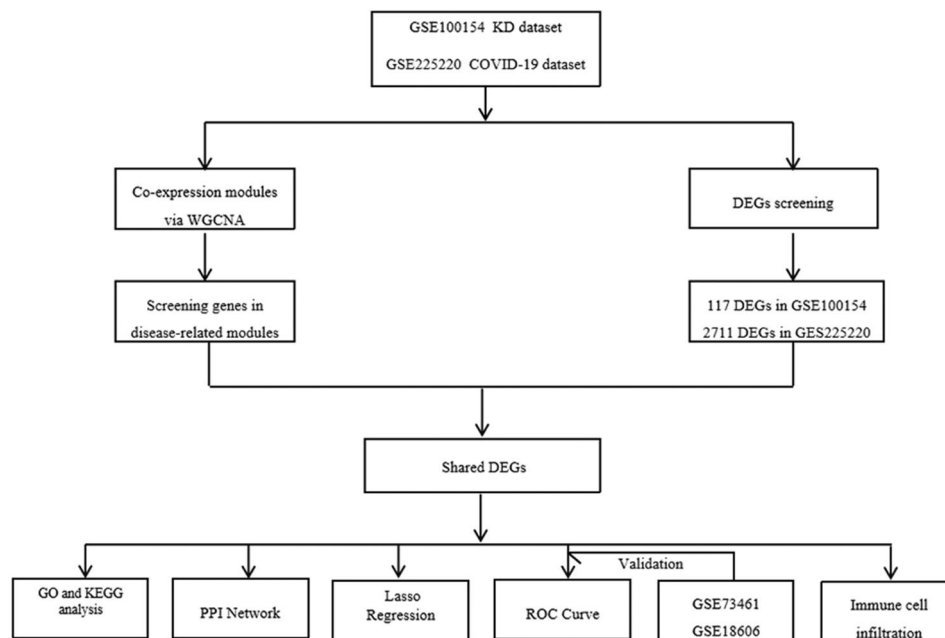


**Fig. 1** Flow chart

**Table 1** RNA expression datasets used in this study

Dataset	Platform	Study Type	Sample Type	N (Control/Cases)*
GSE100154	GPL6884	Expression profiling by array whole blood	44	(23/21)
GSE73461	GPL10558	Expression profiling by array whole blood	133	(55/78)
GSE18606	GPL6480	Expression profiling by array whole blood	22	(11/11)
GSE225220	GPL24676	Expression profiling by high throughput sequencing	63	(26/37)

\* N (Control/Cases): number of subjects used in the current analysis. Three datasets (GSE73461, GSE18606, GSE225220) also included data from additional patients who had other diseases

best soft powers ( $\beta=18$ ) based on a balance of ‘Scale independence’ and ‘Mean connectivity’. The optimal soft threshold was applied so that the constructed network was infinitely close to the scale-free network characteristics. Last, an adjacency matrix was generated and transformed into a topological overlap matrix (TOM). Then, the nodes of the matrix were methodically arranged into a cluster tree using hierarchical clustering. The gene modules were generated using the R package ‘dynamic-TreeCut’ and differentiated by color based on the optimal value of  $\beta$ . The selection criterion for classification was established as ‘minModuleSize’ of 30.

#### Identification of shared differentially expressed genes

Differentially expressed genes (DEGs) were identified in the GSE100154 dataset using the R package ‘limma’ version 3.56.2 [25]. DEGs were defined by standard criteria (adjusted  $P < 0.05$  and  $|\log_2(\text{fold change})| > 1$ ). The R package ‘DESeq2’ version 1.40.2 [26] was utilized to identify DEGs in GSE225220 using the same standard criteria. Module-DEGs were identified by determining the overlap of core module genes and DEGs in GSE100154 using the R package ‘VennDiagram’ version 1.7.3 [27]. Finally, the shared module-DEGs in GSE100154 and DEGs in GSE225220 were selected as the COVID-19-related KD hub genes for subsequent analysis. GEO2R (an online interactive tool at the GEO website) was employed for data normalization, preprocessing, and identification of DEGs in the patient and control groups of GSE18606.

#### Functional enrichment analysis

After identification of hub genes, the R package ‘cluster-Profiler’ version 4.8.3 [28] was used to conduct a functional enrichment analysis. The Gene Ontology (GO) analysis focuses on the terms of biological process, cellular composition, and molecular function, and the Kyoto Encyclopedia of Genes and Genomes (KEGG) analysis identifies related biological pathways and functions. Only highly enriched terms and pathways ( $P < 0.05$ ) were retained.

### Protein-protein interaction network analysis and selection of hub genes

Studies of protein-protein interaction (PPI) networks are crucial for analyses of functional molecular biology. In this analysis, publicly available databases are used to map inputs to PPI data and identify pathways [29]. The STRING tool, a database for customization of PPI networks and functional characterization of gene sets [30], was used to analyze the networks of the hub genes of COVID-19 that were related to KD, and the minimum required interaction score was set as 0.4. These results were displayed using Cytoscape version 3.9.1 [31]. The core functional modules were analyzed using the Cytoscape Molecular Complex Detection (MCODE) plug-in to detect sub-networks of PPI using standard default parameters (Degree Cutoff: 2, Node Score Cutoff: 0.2, K-Core: 2, Max Depth: 100). The CytoHubba plug-in was employed to achieve a more reliable identification of hub genes in the PPI network. This analysis utilized four algorithms for topological analysis: EPC, MNC, MCC, and Degree. The resulting shared genes were then visualized using the R package 'VennDiagram'.

### Combining LASSO regression analysis with ROC curve analyses for identification of key genes

Least Absolute Shrinkage and Selection Operator (LASSO) regression is a widely used machine learning method for the classification or feature selection of high dimensional data [32]. LASSO compresses the estimated coefficient of redundant predictors to zero by constructing the penalty function, so as to screen variables. It was employed to screen for key genes and improve the diagnosis of KD using the R package 'glmnet' version 4.1.8 [33]. Considering the accuracy and simplicity of the model, a lambda within one standard error of the minimum criteria (lambda.1se) was chosen as the optimal lambda by a 10-fold cross-validation. The diagnostic accuracy of key genes was assessed by receiver operating characteristic (ROC) curve analysis with the R package 'pROC' version 1.18.4 [34], and the GSE73461 dataset was utilized for validation. The expression of pivotal genes in the validation dataset (GSE18606), which has samples from patients with KD before and after IVIG treatment, was also examined. GraphPad Prism 8.0.2 was used to visualize these results.

### Immune infiltration analysis

The immune infiltration status of 22 specific immune cells was analyzed in the GSE100154 and GSE225220 datasets with the R package 'CIBERSORT' version 0.1.0 [35]. To identify the correlation of immune cells with the key genes, Spearman correlation coefficients were calculated with the R package 'corrplot' version 0.92 [36].

## Results

### Identification of disease-related modules by WGCNA

We performed the WGCNA with the KD dataset GSE100154 after exclusion of an outlier sample (cutHeight = 150) from a patient with KD (GSM2672295) to improve the reliability of the analysis (Supplementary Fig. 1). We then determined the optimal soft threshold,  $\beta$  (Fig. 2a), and identified 13 modules that had similar co-expression characteristics using the dynamicTreeCut algorithm (Fig. 2b). Next, we determined the relationships of these modules with the KD phenotype by calculation of Pearson's correlation coefficient (Fig. 2c). In the figure, the pink and purple modules had positive correlations with KD, and the green-yellow and turquoise modules had negative correlations with KD. We then identified 1047 genes within these four modules as disease-related genes for the subsequent analysis (Supplementary Table 1).

### Recognition of shared DEGs

We normalized the GSE100154 dataset (Fig. 3a) and the GSE225220 dataset (Fig. 3c), and then identified 117 significant DEGs in GSE100154 (Fig. 3b) and 2711 significant DEGs in GSE225220 (Fig. 3d). Analysis of the WGCNA module (WGCNA\_genes) and DEGs in the GSE100154 dataset (GSE100154\_degs) showed there were 56 shared genes, (Fig. 3e). Further analysis of these 56 genes (GSE100154\_deg\_WGCNA) and the significant DEGs in the GSE225220 dataset (GSE225220\_deg) identified 26 shared genes (Fig. 3f, Supplementary Table 2). We considered these 26 genes to be COVID-19-related KD hub genes.

### Functional annotation of hub genes

We then used the "clusterProfiler" package to perform GO analysis (Fig. 4a) and KEGG analysis (Fig. 4b) of the COVID-19-related KD hub genes. These hub genes had significant enrichment in terms for antimicrobial and immune responses, including "defense response to bacterium", "innate immune response in mucosa", "mucosal immune response", and "neutrophil extracellular trap (NET) formation".

### PPI network analysis

We performed PPI network analysis to examine the interactions among proteins by using the STRING tool, with a focus on COVID-19-related KD hub genes. The resulting network consisted of 26 nodes and 129 edges (Fig. 5a). Then, analysis with the 'MCODE' plug-in of Cytoscape led to the identification of 15 central genes in the most robust module (Fig. 5b). These genes were highly correlated and played a role in a variety of biological processes, including Innate immune response, inflammatory response, neutrophil extracellular trap formation

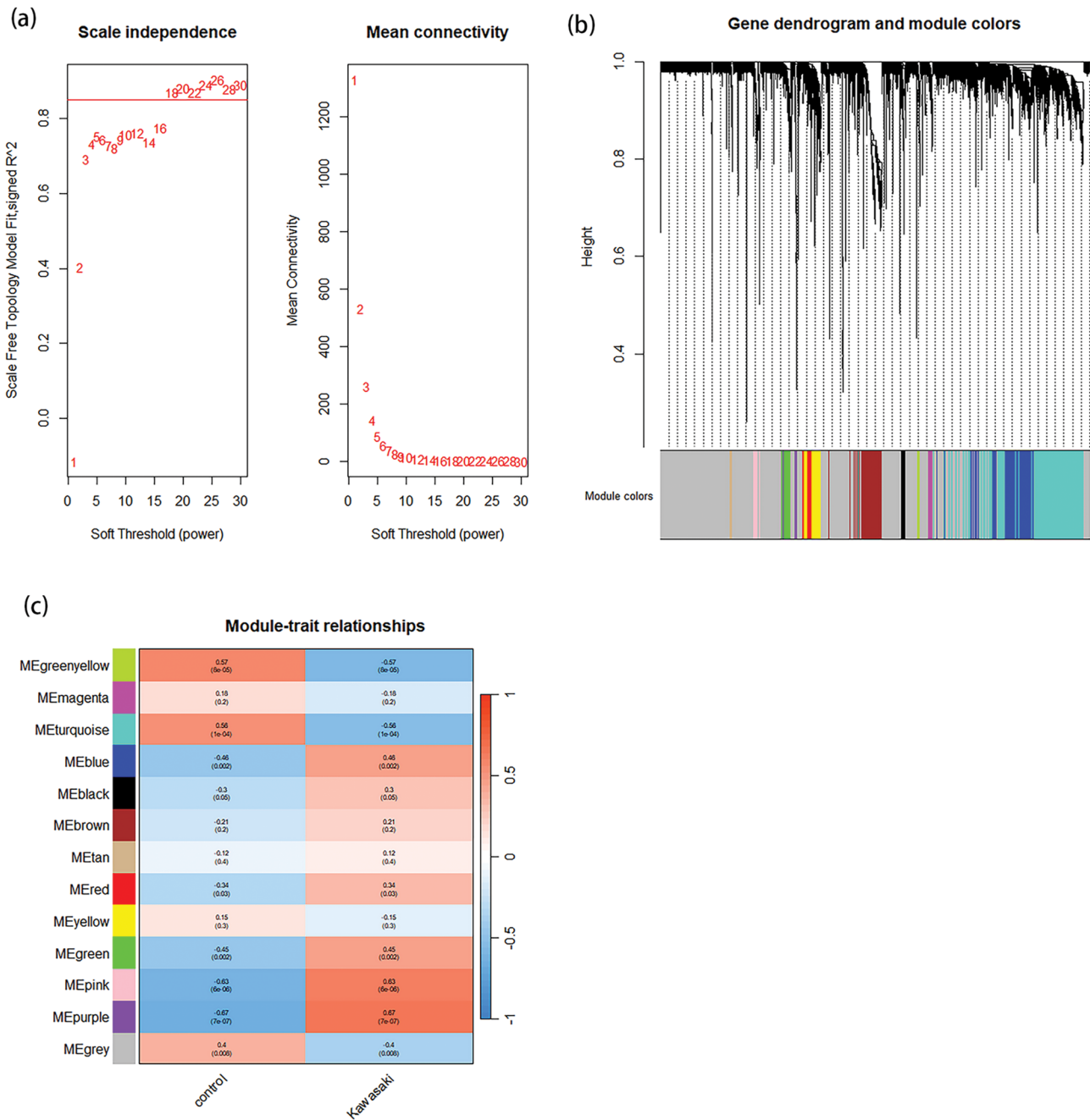


**Fig. 2** WGCNA analysis of the GSE100154 dataset (KD vs. control). **(a)** Network topology for different values of the soft-threshold power, and selection of a  $\beta$  value of 18. **(b)** Gene clustering dendrogram, with different colors indicating distinct clusters. Thirteen modules had similar co-expression characteristics. **(c)** Heatmap for the correlation of different modules with disease phenotype. The pink and purple modules had positive correlations with KD, while the green-yellow and turquoise were negatively correlated

pathway and others. We then implemented four algorithms in cytoHubba (MCC, EPC, Degree, and MNC) for further analysis and identified 9 common hub genes: *MPO*, *LTF*, *CTSG*, *PGLYRP1*, *DEFA4*, *RETN*, *CEACAM8*, *CAMP*, and *AZU1* (Fig. 5c and d).

### Screening of key genes

We performed LASSO regression to further investigate the most reliable marker genes. Based on a  $\lambda_{1se}$  value of 0.1563205, there were three key genes: *DEFA4*, *PGLYRP1*, and *RETN* (Fig. 6a and b). We also calculated the diagnostic value of these three genes by performing ROC curve analysis in the training dataset GSE100154 (Fig. 6c) and the validation dataset GSE73461 (Fig. 6d).

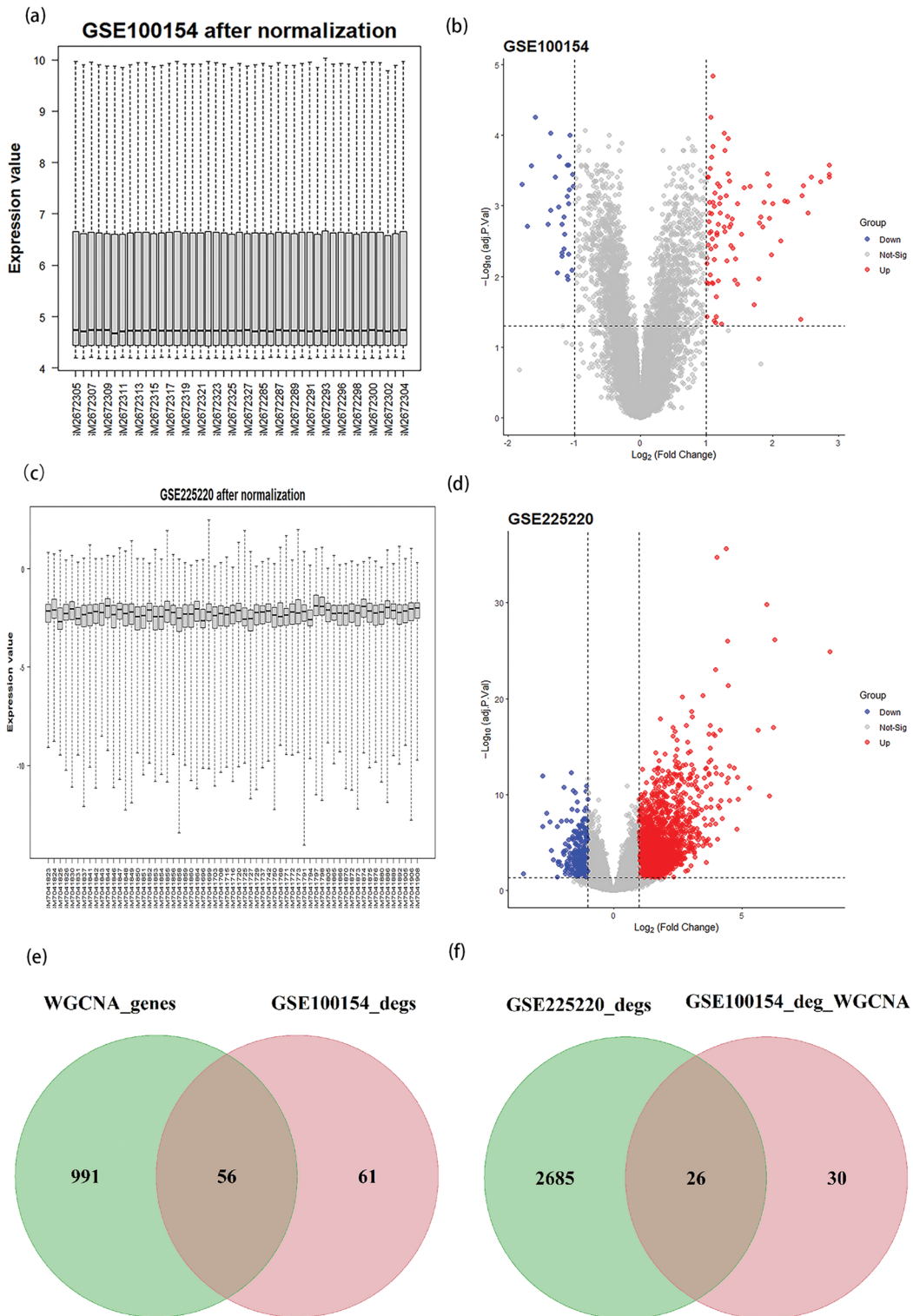


**Fig. 3** Identification of DEGs in the GSE100154 dataset and the GSE225220 dataset. **(a, b)** Data normalization and volcano plot of DEGs in GSE100154(KD vs. control). **(c, d)** Data normalization and volcano plot of DEGs in GSE225220(COVID-19 vs. control). (adj.  $P < 0.05, |\log_2FC| > 1$ ). **(e)** Shared genes in comparison of the WGCNA modules ( $n = 1047$ ) and the DEGs in GSE100154 ( $n = 117$ ). **(f)** Shared genes in comparison of the WGCNA modules and DEGs in GSE100154 ( $n = 56$ ) and the DEGs in GSE225220 ( $n = 2711$ ).  $\log_2FC$ :  $\log_2(\text{fold-change})$

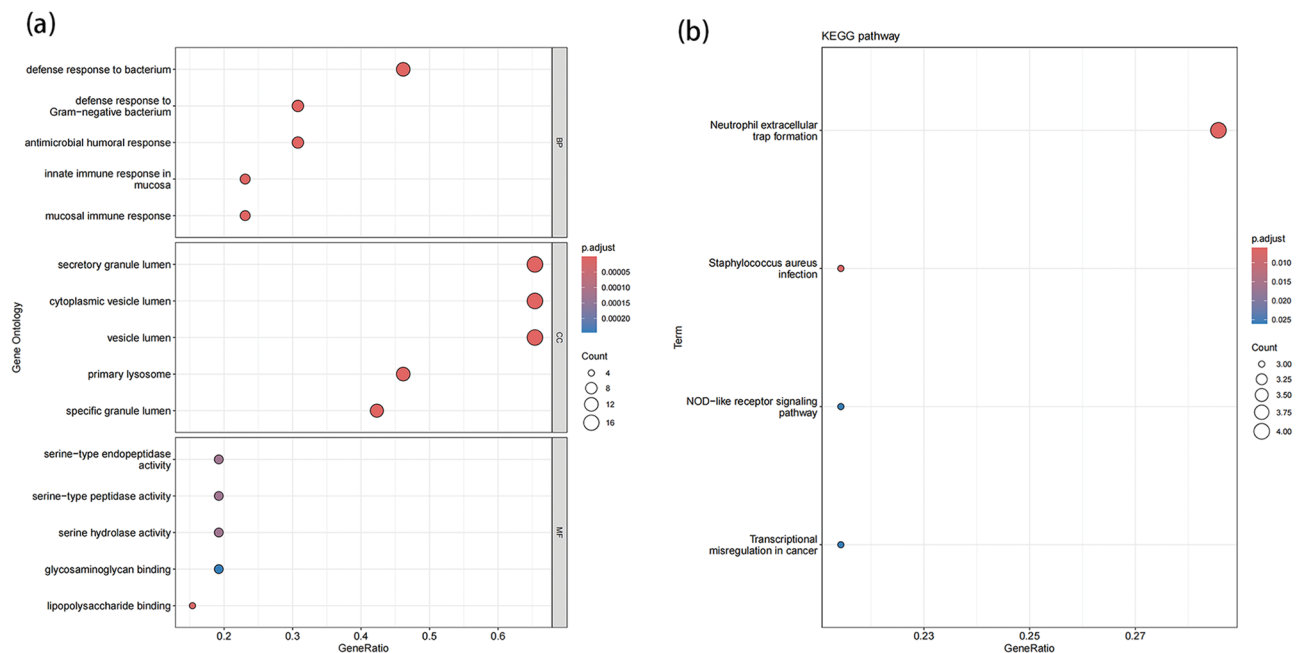


**Fig. 4** Functional enrichment analysis of COVID-19-related KD hub genes. **(a)** The top 5 GO terms related to three categories of hub genes (BP, biological process; CC, cellular component; MF, molecular function). **(b)** KEGG pathways related to the hub genes. Only highly enriched terms and pathways ( $P < 0.05$ ) were retained

For the training dataset, *DEFA4* had an area under the curve (AUC) of 0.885 ( $P = 4.82 \times 10^{-18}$ ), *PGLYRP1* had an AUC 0.870 ( $P = 5.39 \times 10^{-6}$ ), and *RETN* had an AUC of 0.872 ( $P = 4.67 \times 10^{-6}$ ). For the validation dataset *DEFA4* had an AUC of 0.748 ( $P = 6.04 \times 10^{-7}$ ), *PGLYRP1* had an AUC of 0.938 ( $P = 4.82 \times 10^{-18}$ ), and *RETN* had an AUC of 0.961 ( $P = 7.87 \times 10^{-20}$ ).

Our subsequent analysis of the GSE100154 dataset clearly demonstrated that the levels of these three mRNAs were expressed at significantly greater levels in patients with KD than in healthy controls (Fig. 7a, Supplementary Fig. 2). In agreement, the expression of *PGLYRP1* and *RETN* were significantly lower after IVIG treatment of patients with acute KD from the GSE18606 dataset (Fig. 7b, Supplementary Table 3). Taken together, these results indicated that *DEFA4*, *PGLYRP1*, and *RETN* were potential key hub genes of KD that were also associated with COVID-19.

### Immune infiltration analysis

As described above, the COVID-19-related KD hub genes were mostly enriched in inflammation and immunity (“defense response to bacterium”, “innate immune response in mucosa”, and “mucosal immune response” and “NET formation”). We therefore analyzed the infiltration of 22 types of immune cells in the GSE100154 dataset, which compares patients with KD and healthy controls (Fig. 8a) and the GSE225220 dataset, which compares patients with COVID-19 to healthy controls (Fig. 8b). Relative to the controls, patients with KD had

significantly greater infiltration of activated dendritic cells (DCs), M0 macrophages, and monocytes but less infiltration of CD8 T cells, T regulatory cells (Tregs), resting mast cells, and resting natural killer (NK) cells (Fig. 8c). Relative to the controls, COVID-19 patients had significantly greater infiltration of naive B cells and M0 macrophages, but less infiltration of resting NK cells, plasma cells, resting T cells, CD4 memory cells, and naive CD4 T cells (Fig. 8d).

We then performed Spearman correlation analysis to determine the relationships of *DEFA4*, *PGLYRP1*, and *RETN* with immune cell infiltration in patients with COVID-19 (Fig. 8e) and patients with KD (Fig. 8f). The comparison of patients with KD to controls showed that all three of these key genes had strong positive correlations with M0 macrophages, activated DCs, and Tregs, and significant negative correlations with CD8 T cells. In addition, a comparison of patients with COVID-19 to controls showed that all three of these genes also had very strong negative correlations with resting CD4 memory T cells.

### Discussion

KD is an acute vasculitis that predominantly affects children and has no clearly defined cause<sup>1</sup>. Some earlier research indicated that KD might be caused by a novel RNA virus [37, 38], possibly the HCoV NL63 virus [39], but subsequent evidence proved otherwise [40]. The COVID-19 pandemic led to renewed interest in studying viral agents as possible causes of KD. Patients with

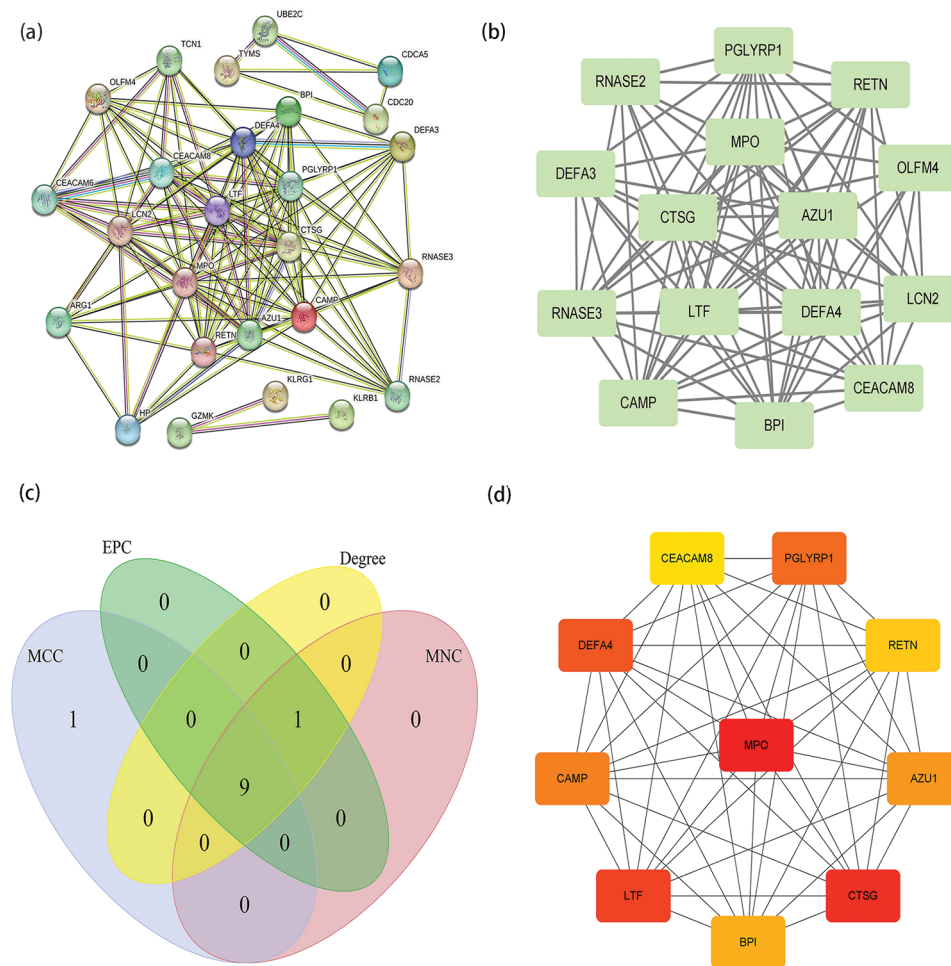


**Fig. 5** PPI network analysis of COVID-19-related KD hub genes. **(a)** PPI network of 26 hub genes. **(b)** Fifteen genes in the most representative module screened by the 'MCODE' plug-in. **(c)** Common hub genes identified from four algorithms of cytoHubba (MCC, EPC, Degree and MNC). **(d)** Network of the nine common hub genes. MCC: Maximal Clique Centrality, EPC: Edge Percolated Component, MNC: Maximum Neighborhood Component

COVID-19 and with KD often exhibit some of the same clinical symptoms, including fever, rash, and conjunctivitis [41, 42]. Pediatric inpatients who are diagnosed with COVID-19 most often present with mild clinical features [43, 44]. Nevertheless, several weeks after infection with SARS-CoV-2, certain children experience a disorder with symptoms that resemble KD [45, 46], although the molecular basis of this condition remains uncertain. Therefore, our aim was to examine possible similarities in the molecular pathogenesis and pathways of these two diseases.

We initially identified four significant modules associated with the KD phenotype (Fig. 2c), which consisted of two positive modules (purple and pink) and two negative modules (green-yellow and turquoise). To achieve more reliable results from bioinformatics studies, many recent studies screen biomarkers by integrating WGCNA and DEG analyses [47, 48]. We therefore cross-analyzed the genes of the four modules with 117 DEGs in KD from the GSE100154 dataset, and obtained 56 candidate genes

(Fig. 3e). We then identified 26 shared genes in COVID-19 and KD (Fig. 3f). These genes have potential as molecular targets for novel therapies for KD and COVID-19.

Our functional annotation analyses showed that these candidate genes were associated with defense responses to bacteria, innate immune responses in mucosal tissues, and mucosal immune responses, and that these genes may exert their functions through pathways such as NETs, *Staphylococcus aureus* infection, and the NOD-like receptor signaling pathway. Of the 26 shared genes, six were enriched on the biological process of innate immune response, including DEFA3, DEFA4, CAMP, RNASE2, RNASE3, LTF. Recent research suggested that pathogen-associated molecular patterns associated with innate immunity could cause vasculitis, which may be related to the pathogenesis of KD [49]. Patients with COVID-19 have increased levels of neutrophils, C-reactive protein (CRP), and other inflammatory markers [45, 50, 51], and also have abnormal immune responses, particularly alterations in T lymphocytes [52]. Inflammation

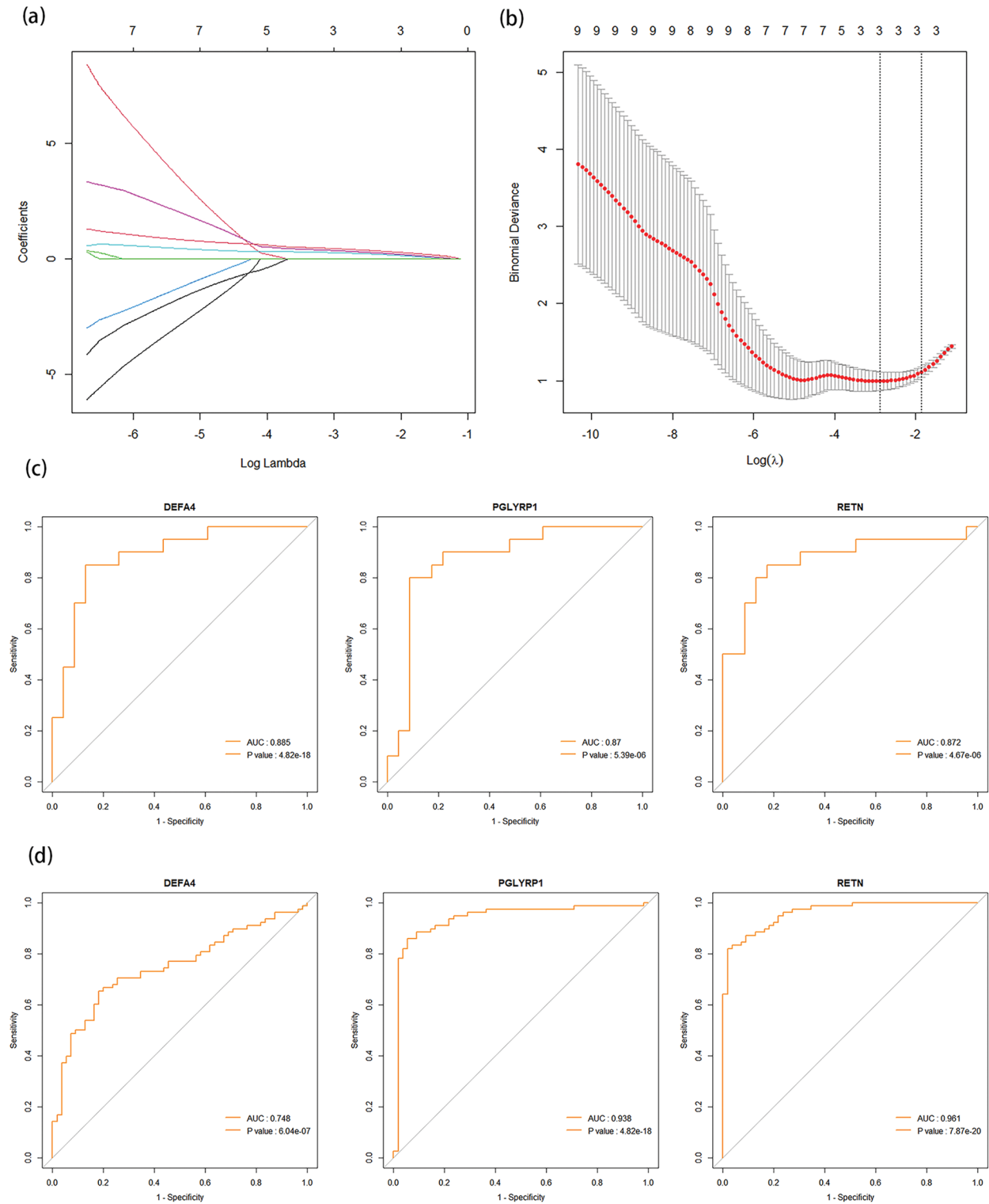


**Fig. 6** Identification of the key COVID-19-related KD hub genes. **(a, b)** Screening of *DEFA4*, *PGLYRP1*, and *RETN* by LASSO regression analysis. The optimal lambda ( $\lambda_{1se}$ ) was 0.1563205 based on a 10-fold cross-validation. **(c)** ROC curves of *DEFA4*, *PGLYRP1*, *RETN* in the training dataset (GSE100154, KD vs. control). **(d)** ROC curves of *DEFA4*, *PGLYRP1*, and *RETN* in the validation dataset (GSE73461, KD vs. control). AUC: area under the curve

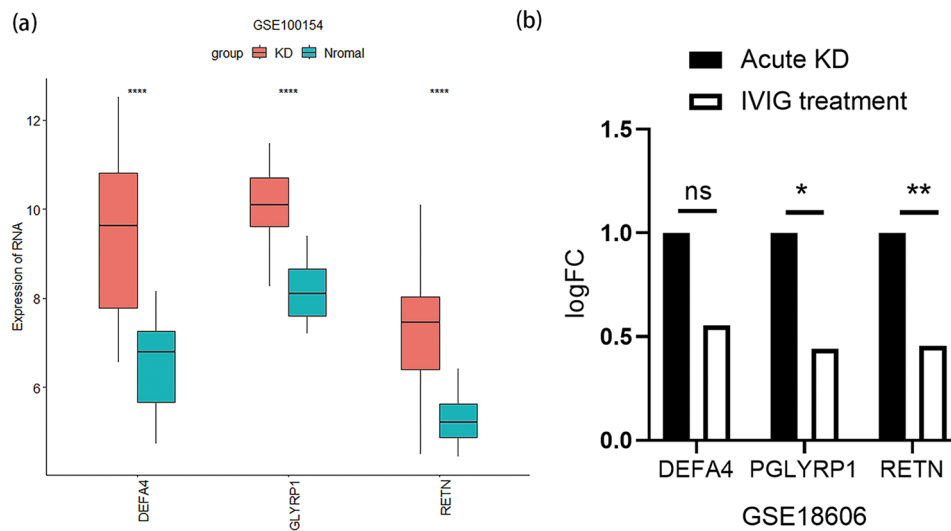


**Fig. 7** Validation of the expression of the key COVID-19-related KD hub genes. **(a)** Expression of *DEFA4*, *PGLYRP1*, and *RETN* in the GSE100154 dataset (KD vs. control). **(b)** Expression of *DEFA4*, *PGLYRP1*, and *RETN* in KD patients before and after IVIG treatment in the GSE18606 dataset. \* $p < 0.05$ ; \*\* $p < 0.01$ ; \*\*\* $p < 0.001$ ; \*\*\*\* $p < 0.0001$ . logFC:  $\log_2$ (fold-change)

and an excessive immune response also occur in KD [53, 54]. Moreover, the activation of NETs triggers vascular endothelial growth factor A and hypoxia-inducible factor-1 $\alpha$ , which are involved in the pathogenesis of KD, and other evidence demonstrated that targeting of NETs can lead to a notable rise in the activation of PI3K and Akt [55]. These previous findings underscore the importance of our study of the regulation of inflammatory immune responses and the genes potentially associated with both COVID-19 and KD.

Our PPI analysis showed that there were nine central genes among the potential COVID-19-related KD hub genes (Fig. 5d): *MPO*, *LTF*, *CTSG*, *PGLYRP1*, *DEFA4*, *RETN*, *CEACAM8*, *CAMP*, and *AZU1*. Our subsequent LASSO regression analysis showed that three of these nine hub genes had enhanced predictive and diagnostic value for both COVID-19 and KD: *DEFA4*, *PGLYRP1*, and *RETN*. LASSO is a regression analysis method that compresses the estimated variables by adding penalty parameters to the least squares regression, thereby improving the prediction accuracy of the model [56]. We therefore used this method to select the best predictive variables. Currently, LASSO has been widely used for model construction, such as the early diagnosis of KD, and for a bronchial dysplasia prediction model, which have shown good prediction effect and stability [57, 58]. ROC curve analysis of the training data and the validation data confirmed the diagnostic significance of these three genes. Moreover, these three genes had increased expression in patients with KD relative to healthy controls, and *PGLYRP1* and *RETN* were down-regulated after IVIG treatment of patients with KD, indicating their potential as biomarkers for COVID-19-related KD.

Defensin alpha 4 (*DEFA4*) is in the alpha defensin family and is an antimicrobial peptide and component of the innate immune system. Neutrophils express *DEFA4*, and this peptide can combat infections by Gram-negative bacteria and viruses [59–61]. There is evidence that the levels of *DEFA4* and other genes are positively correlated with the severity of symptoms in patients infected by viruses [62], including in patients with COVID-19 [63] and with certain autoimmune disorders [64, 65], although the present study is the first to report it may also have a role in the pathogenesis of KD.

Peptidoglycan recognition protein 1 (*PGLYRP1*) is an innate immune activator that has antibacterial activity [66], and its expression is closely associated with inflammatory responses. Notably, *PGLYRP1* appears to have different effects in different diseases. At the molecular level, tumor necrosis factor receptor 1 (TNFR1) functions in the regulation of proinflammatory cytokines, and *PGLYRP1* binds to TNFR1 and thereby obstructs the TNF- $\alpha$ -induced death in tumor cells [67, 68]. Other investigations revealed that two short peptides derived from *PGLYRP1* (17.1 and N1) suppressed the inflammatory response in a mouse model of acute lung injury, suggesting they may have potential as treatments for inflammatory lung diseases, including COVID-19 [69]. The level of *PGLYRP1* is also elevated in patients with rheumatoid arthritis, indicating its potential as a diagnostic marker for the severity of this autoimmune disease [70]. Ruxolitinib is a Janus kinase inhibitor that has demonstrated effectiveness in treating severe and critical cases of COVID-19, and this drug also decreases *PGLYRP1* levels [71]. Importantly, our results

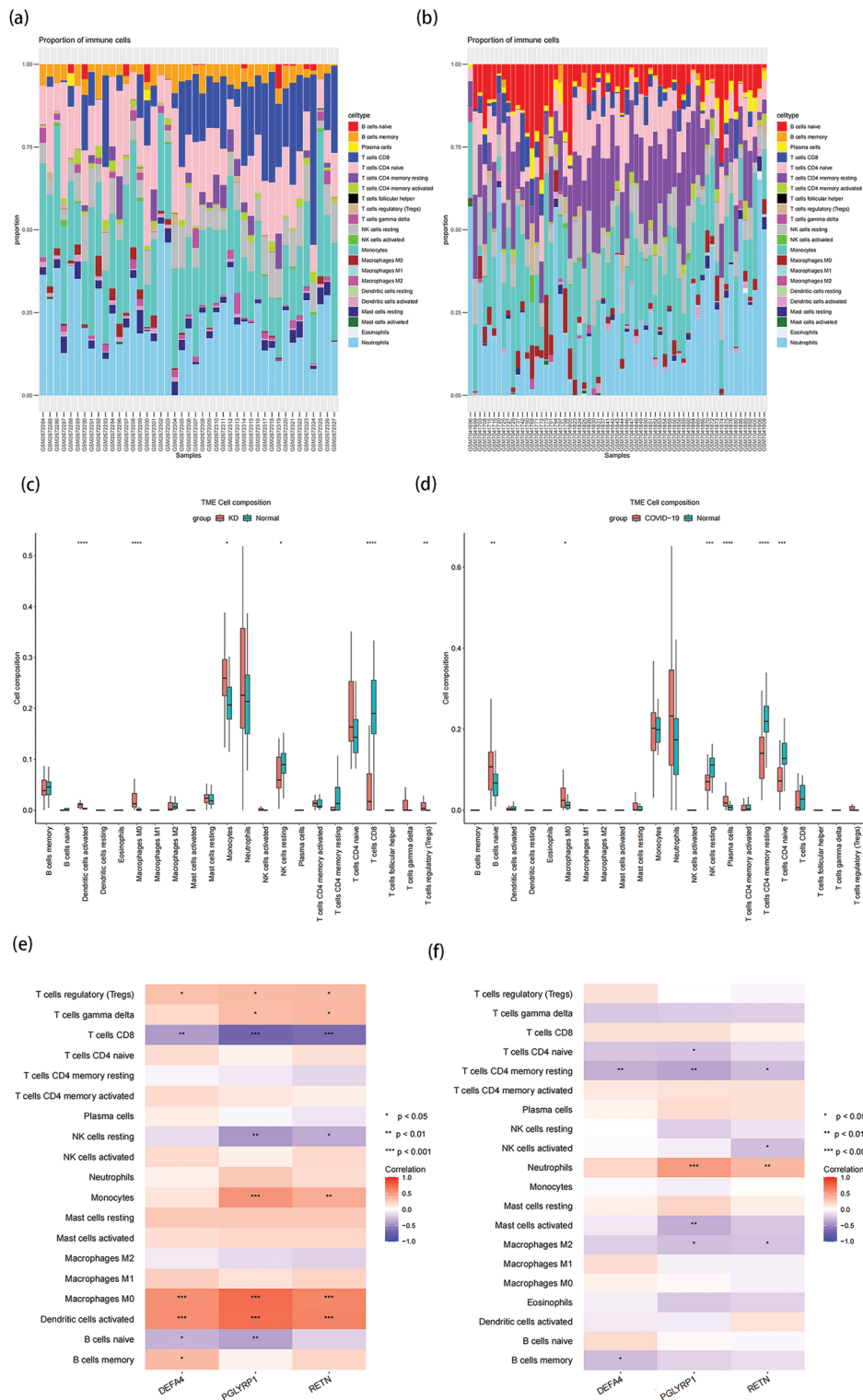


**Fig. 8** Relationship of immune cell infiltration and key COVID-19-related KD hub genes. **(a)** Proportions of 22 types of immune cells in each sample of the GSE100154 dataset (KD vs. control). **(b)** Proportions of 22 types of immune cells in each sample of the GSE225220 dataset (COVID-19 vs. control). **(c)** Infiltration status of immune cells in the two groups of the GSE100154 dataset. **(d)** Infiltration status of immune cells in the two groups of the GSE225220 dataset. **(e)** Correlation of *DEFA4*, *PGLYRP1*, and *RETN* with infiltration of different immune cells in the GSE100154 dataset. **(f)** Correlation of *DEFA4*, *PGLYRP1*, and *RETN* with infiltration of different immune cells in the GSE225220 dataset. \* $p < 0.05$ ; \*\* $p < 0.01$ ; \*\*\* $p < 0.001$

demonstrated higher levels of *PGLYRP1* in COVID-19 and KD samples compared to the healthy control groups.

Resistin (RETN) is a type of adipocytokine that occurs in fat cells, and it acquired its name because initial studies showed that intravenous RETN can lead to insulin resistance in mice [72]. An elevated level of RETN may also be linked to immune system activation in patients with acute KD [73]. Furthermore, studies of patients with diabetes showed that the level of RETN had a positive correlation with the level of CRP [74, 75]. Although changes in the level of RETN occur during SARS-CoV infection, further investigation of this topic is warranted [76].

Inflammatory responses and excessive immune responses occur during the pathological processes of both COVID-19 and KD, and excessive inflammation with potentially fatal consequences can occur due to the dysregulation of immune function [77]. The levels of T cells and NK cells are decreased in patients with COVID-19 with more severe symptoms [51, 52], and macrophages are also a pivotal factor related to the severity of COVID-19 [78]. Similarly, patients with acute KD have decreased activation of T cells in the peripheral blood [79], and some research suggested that the abnormal stimulation of monocytes and macrophages may be linked to the formation of vascular lesions in KD [80]. Our results showed that patients with KD had increased levels of monocytes, M0 macrophages, and DCs, which had been confirmed in some previous studies, and may explain the role of innate immune response in KD [81, 82]. In addition, we found that the level of CD8 T cells decreased in the KD group, which was consistent with previous studies [83, 84]. CD8 T cells can inhibit the immune response of CD4 cells. Inhibition of CD8 cells promotes the excessive activation of cellular immunity and promote inflammatory damage of the vascular wall. In addition, we also found that patients with COVID-19 had higher levels of M0 macrophages and a lower level of CD4 T cells relative to healthy controls (Fig. 8). CD4 T cells can be used to assess the severity of COVID-19 in patients. Patients with KD also had significant correlations in the levels of the three key genes (*DEFA4*, *PGLYRP1*, and *RETN*) with these different types of immune cells. Consequently, these three key genes may function as immunomodulation nodes for COVID-19-related KD. Currently, there are two clinical obstacles are to be concerned about: early diagnosis and unresponsiveness to IVIG treatment in KD [85, 86]. Our finding may provide a new perspective of molecular immune mechanisms to the diagnosis and therapy in KD. However, we need to stress that our bioinformatics approach was limited, and LASSO may randomly select one and ignore others if there are highly correlated variables, leading to selection bias. Or when the number of features is much larger than the sample size, Lasso regression would not

be the first choice. These problems may be corrected by combination with other methods, such as Random Forest. The sample size of the KD and COVID-19 group was not completely balanced, and different microarray platforms may produce potential bias. For example, because of the different preprocessing methods of GEO data sets on different platforms, there may be potential bias on the results due to statistical methods. Moreover, the information provided by different platforms varies greatly, and the basic clinical characteristics of patients may not match, reducing the interpretability of the results. In addition, we only provided a theoretical verification of these screened biomarkers. Therefore, in future studies, in addition to verify the expression of these key markers in vitro, we will also construct a diagnostic model of KD based on these hubs and immune-related indicators, such as T cells, and verify it in a large cohort.

## Conclusions

In summary, we identified three novel genes that function in the immunomodulatory responses of patients with COVID-19 and KD patients: *DEFA4*, *PGLYRP1*, and *RETN*. Future studies of these genes may further elucidate the pathogenic mechanisms of these diseases and lead to targeted treatments.

## Abbreviations

COVID-19	Coronavirus Disease 2019
KD	Kawasaki Disease
DEGs	Differentially Expressed Genes
LASSO	Least Absolute Shrinkage and Selection Operator
WGCNA	Weighted Gene Co-Expression Network Analysis
CALs	Coronary Artery Lesions
GEO	Gene Expression Omnibus
GO	Gene Ontology
KEGG	Kyoto Encyclopedia of Genes and Genomes
PPI	Protein-Protein Interaction
ROC	Receiver Operating Characteristic

## Supplementary Information

The online version contains supplementary material available at <https://doi.org/10.1186/s12887-025-05752-z>.

Supplementary Material 1

Supplementary Material 2

Supplementary Material 3

Supplementary Material 4

Supplementary Material 5

## Acknowledgements

We are grateful to the developers of the Gene Expression Omnibus (GEO) database and of R software and its many packages. This paper was supported by the Guangdong Basic and Applied Basic Research Foundation (2019A1515110073).

## Author contributions

Conception and design: W.L.; Data checking: W.Z and X.T.; Manuscript writing: W.L.; Editing and revision: Z.P and J.Y.; Supervision: S.N.; Final approval of the manuscript: all authors.

**Funding**

This study was funded by the GuangDong Basic and Applied Basic Research Foundation (2019A1515110073).

**Data availability**

The datasets generated during and/or analysed during the current study are available from the corresponding author on reasonable request.

**Declarations****Ethics approval and consent to participate**

Not applicable.

**Consent for publication**

Not applicable.

**Competing interests**

The authors declare no competing interests.

Received: 22 March 2024 / Accepted: 8 May 2025

Published online: 19 May 2025

**References**

- Ozen S, et al. EULAR/PRES endorsed consensus criteria for the classification of childhood vasculitides. *Ann Rheum Dis*. 2006;65(7):936–41. <https://doi.org/10.1136/ard.2005.046300>.
- Newburger JW, et al. Diagnosis, treatment, and long-term management of Kawasaki disease: a statement for health professionals from the committee on rheumatic fever, endocarditis and Kawasaki disease, Council on cardiovascular disease in the young. *Am Heart Association Circulation*. 2004;110(17):2747–71. <https://doi.org/10.1161/01.cir.0000145143.19711.78>.
- McCordle BW, et al. Diagnosis, treatment, and Long-Term management of Kawasaki disease: A scientific statement for health professionals from the American heart association. *Circulation*. 2017;135(17):e927–99. <https://doi.org/10.1161/cir.0000000000000484>.
- Nakamura Y, et al. Epidemiologic features of Kawasaki disease in Japan: results of the 2009–2010 nationwide survey. *J Epidemiol*. 2012;22(3):216–21. <https://doi.org/10.2188/jea.20110126>.
- Hamden A, Tulloh R, Burgner D. Kawasaki disease. *BMJ*. 2014;349:g5336. <https://doi.org/10.1136/bmj.g5336>.
- Burns JC, et al. Seasonality and Temporal clustering of Kawasaki syndrome. *Epidemiology*. 2005;16(2):220–5. <https://doi.org/10.1097/01.ede.0000152901.06689.d4>.
- Kim GB, et al. Epidemiologic features of Kawasaki disease in South Korea: data from nationwide survey, 2009–2011. *Pediatr Infect Dis J*. 2014;33(1):24–7. <https://doi.org/10.1097/inf.0000000000000010>.
- Lue HC, et al. Epidemiological features of Kawasaki disease in Taiwan, 1976–2007: results of five nationwide questionnaire hospital surveys. *Pediatr Neonatol*. 2014;55(2):92–6. <https://doi.org/10.1016/j.pedneo.2013.07.010>.
- Ae R, et al. Epidemiology, treatments, and cardiac complications in patients with Kawasaki disease: the nationwide survey in Japan, 2017–2018. *J Pediatr*. 2020;225:23–e2922. <https://doi.org/10.1016/j.jpeds.2020.05.034>.
- Xie LP, et al. Epidemiologic features of Kawasaki disease in Shanghai from 2013 through 2017. *J Epidemiol*. 2020;30(10):429–35. <https://doi.org/10.2188/jea.JE20190065>.
- Du ZD, et al. Epidemiologic study on Kawasaki disease in Beijing from 2000 through 2004. *Pediatr Infect Dis J*. 2007;26(5):449–51. <https://doi.org/10.1097/01.inf.0000261196.79223.18>.
- Burns JC, Glodé MP. Kawasaki syndrome. *Lancet*. 2004;364(9433):533–44. [https://doi.org/10.1016/s0140-6736\(04\)16814-1](https://doi.org/10.1016/s0140-6736(04)16814-1).
- Sohn MH, Noh SY, Chang W, Shin KM, Kim DS. Circulating Interleukin 17 is increased in the acute stage of Kawasaki disease. *Scand J Rheumatol*. 2003;32(6):364–6. <https://doi.org/10.1080/03009740410005034>.
- Shulman ST, Rowley AH. Kawasaki disease: insights into pathogenesis and approaches to treatment. *Nat Rev Rheumatol*. 2015;11(8):475–82. <https://doi.org/10.1038/nrrheum.2015.54>.
- Rowley AH, Shulman ST. The epidemiology and pathogenesis of Kawasaki disease. *Front Pediatr*. 2018;6:374. <https://doi.org/10.3389/fped.2018.00374>.
- Lu R, et al. Genomic characterisation and epidemiology of 2019 novel coronavirus: implications for virus origins and receptor binding. *Lancet*. 2020;395(10224):565–74. [https://doi.org/10.1016/s0140-6736\(20\)30251-8](https://doi.org/10.1016/s0140-6736(20)30251-8).
- Finkel Y, et al. The coding capacity of SARS-CoV-2. *Nature*. 2021;589(7840):125–30. <https://doi.org/10.1038/s41586-020-2739-1>.
- Galván Casas C, et al. Classification of the cutaneous manifestations of COVID-19: a rapid prospective nationwide consensus study in Spain with 375 cases. *Br J Dermatol*. 2020;183(1):71–7. <https://doi.org/10.1111/bjd.19163>.
- Verdoni L, et al. An outbreak of severe Kawasaki-like disease at the Italian epicentre of the SARS-CoV-2 epidemic: an observational cohort study. *Lancet*. 2020;395(10239):1771–8. [https://doi.org/10.1016/s0140-6736\(20\)31103-x](https://doi.org/10.1016/s0140-6736(20)31103-x).
- Viner RM, Whittaker E. Kawasaki-like disease: emerging complication during the COVID-19 pandemic. *Lancet*. 2020;395(10239):1741–3. [https://doi.org/10.1016/s0140-6736\(20\)31129-6](https://doi.org/10.1016/s0140-6736(20)31129-6).
- European Centre for Disease Prevention and Control. Pediatric inflammatory multisystem syndrome and SARS-CoV-2 infection in children– 15 May 2020. ECDC: Stockholm. (2020).
- Medaglia AA, et al. Kawasaki disease recurrence in the COVID-19 era: a systematic review of the literature. *Ital J Pediatr*. 2021;47(1):95. <https://doi.org/10.1186/s13052-021-01041-4>.
- Rivera-Figueroa EI, Santos R, Simpson S, Garg P. Incomplete Kawasaki disease in a child with Covid-19. *Indian Pediatr*. 2020;57(7):680–1. <https://doi.org/10.1007/s13312-020-1900-0>.
- Langfelder P, Horvath S. WGCNA: an R package for weighted correlation network analysis. *BMC Bioinformatics*. 2008;9:559. <https://doi.org/10.1186/1471-2105-9-559>.
- Ritchie ME, et al. Limma powers differential expression analyses for RNA-sequencing and microarray studies. *Nucleic Acids Res*. 2015;43(7):e47. <https://doi.org/10.1093/nar/gkv007>.
- Love MI, Huber W, Anders S. Moderated Estimation of fold change and dispersion for RNA-seq data with DESeq2. *Genome Biol*. 2014;15(12):550. <https://doi.org/10.1186/s13059-014-0550-8>.
- Chen H, Boutros PC. VennDiagram: a package for the generation of highly-customizable Venn and Euler diagrams in R. *BMC Bioinformatics*. 2011;12:35. <https://doi.org/10.1186/1471-2105-12-35>.
- Yu G, Wang LG, Han Y, He QY. ClusterProfiler: an R package for comparing biological themes among gene clusters. *Omic*. 2012;16(5):284–7. <https://doi.org/10.1089/omi.2011.0118>.
- Liu G, Wong L, Chua H. N. Complex discovery from weighted PPI networks. *Bioinformatics*. 2009;25(15):1891–7. <https://doi.org/10.1093/bioinformatics/btp311>.
- Szklarczyk D et al. The STRING database in 2021: customizable protein-protein networks, and functional characterization of user-uploaded gene/measurement sets. *Nucleic Acids Res*. 49(D1), D605–d612 (2021). <https://doi.org/10.1093/nar/gkaa1074>
- Lotia S, Montojo J, Dong Y, Bader GD, Pico AR. Cytoscape app store. *Bioinformatics*. 2013;29(10):1350–1. <https://doi.org/10.1093/bioinformatics/btt138>.
- Xue F, Yang L, Dai B, et al. Bioinformatics profiling identifies seven immune-related risk signatures for hepatocellular carcinoma. *PeerJ*. 2020;8:e8301. <https://doi.org/10.7717/peerj.8301>.
- Engelbrecht S, Bohlin J. Statistical predictions with Glimnet. *Clin Epigenetics*. 2019;11(1):123. <https://doi.org/10.1186/s13148-019-0730-1>.
- Robin X, et al. pROC: an open-source package for R and S+ to analyze and compare ROC curves. *BMC Bioinformatics*. 2011;12:77. <https://doi.org/10.1186/1471-2105-12-77>.
- Zhao ECIBERSORT. Cell-type Identification By Estimating Relative Subsets Of RNA Transcripts. R package version 0.1.0. (2023).
- Wei T, Simko V. R package 'corrplot': Visualization of a Correlation Matrix (Version 0.92). Available from <https://github.com/taiyun/corrplot>. (2021).
- Rowley AH, et al. Ultrastructural, Immunofluorescence, and RNA evidence support the hypothesis of a new virus associated with Kawasaki disease. *J Infect Dis*. 2011;203(7):1021–30. <https://doi.org/10.1093/infdis/jiq136>.
- Rowley AH, et al. RNA-containing cytoplasmic inclusion bodies in ciliated bronchial epithelium months to years after acute Kawasaki disease. *PLoS ONE*. 2008;3(2):e1582. <https://doi.org/10.1371/journal.pone.0001582>.
- Esper F, et al. Association between a novel human coronavirus and Kawasaki disease. *J Infect Dis*. 2005;191(4):499–502. <https://doi.org/10.1086/428291>.
- Rowley AH. Finding the cause of Kawasaki disease: a pediatric infectious diseases research priority. *J Infect Dis*. 2006;194(12):1635–7. <https://doi.org/10.1086/509514>.

41. Gottlieb M, Long B. Dermatologic manifestations and complications of COVID-19. *Am J Emerg Med*. 2020;38(9):1715–21. <https://doi.org/10.1016/j.ajem.2020.06.011>.
42. Loffredo L, et al. Conjunctivitis and COVID-19: A meta-analysis. *J Med Virol*. 2020;92(9):1413–4. <https://doi.org/10.1002/jmv.25938>.
43. Ma X, et al. The clinical characteristics of pediatric inpatients with SARS-CoV-2 infection: A meta-analysis and systematic review. *J Med Virol*. 2021;93(1):234–40. <https://doi.org/10.1002/jmv.26208>.
44. Dong Y, et al. Epidemiology of COVID-19 among children in China. *Pediatrics*. 2020;145(6). <https://doi.org/10.1542/peds.2020-0702>. e20200702.
45. Chen N, et al. Epidemiological and clinical characteristics of 99 cases of 2019 novel coronavirus pneumonia in Wuhan, China: a descriptive study. *Lancet*. 2020;395(10223):507–13. [https://doi.org/10.1016/s0140-6736\(20\)30211-7](https://doi.org/10.1016/s0140-6736(20)30211-7).
46. Zhu YP, et al. Immune response to intravenous Immunoglobulin in patients with Kawasaki disease and MIS-C. *J Clin Invest*. 2021;131(20). <https://doi.org/10.1172/jci147076>. e147076.
47. Yuan Y, Li N, Fu M, Ye M. Identification of critical modules and biomarkers of ulcerative colitis by using WGCNA. *J Inflamm Res*. 2023;16:1611–28. <https://doi.org/10.2147/jir.s402715>.
48. Zhang M, Ke B, Zhuo H, Guo B. Diagnostic model based on bioinformatics and machine learning to distinguish Kawasaki disease using multiple datasets. *BMC Pediatr*. 2022;22(1):512. <https://doi.org/10.1186/s12887-022-03557-y>.
49. Hara T, et al. Kawasaki disease: a matter of innate immunity. *Clin Exp Immunol*. 2016;186(2):134–43. <https://doi.org/10.1111/cei.12832>.
50. Wu F, et al. A new coronavirus associated with human respiratory disease in China. *Nature*. 2020;579(7798):265–9. <https://doi.org/10.1038/s41586-020-2008-3>.
51. Ouyang Y, et al. Downregulated gene expression spectrum and immune responses changed during the disease progression in patients with COVID-19. *Clin Infect Dis*. 2020;71(16):2052–60. <https://doi.org/10.1093/cid/ciaa462>.
52. Qin C, et al. Dysregulation of immune response in patients with coronavirus 2019 (COVID-19) in Wuhan, China. *Clin Infect Dis*. 2020;71(15):762–8. <https://doi.org/10.1093/cid/ciaa248>.
53. Matsubara T, Ichiyama T, Furukawa S. Immunological profile of peripheral blood lymphocytes and monocytes/macrophages in Kawasaki disease. *Clin Exp Immunol*. 2005;141(3):381–7. <https://doi.org/10.1111/j.1365-2249.2005.02821.x>.
54. Furuno K, et al. CD25 + CD4 + regulatory T cells in patients with Kawasaki disease. *J Pediatr*. 2004;145(3):385–90. <https://doi.org/10.1016/j.jpeds.2004.05.048>.
55. Jing Y, et al. Neutrophil extracellular trap from Kawasaki disease alter the biologic responses of PBMC. *Biosci Rep*. 2020;40(9):BSR20200928. <https://doi.org/10.1042/bsr20200928>.
56. Cecelja M, et al. Genetic aetiology of blood pressure relates to aortic stiffness with bi-directional causality: evidence from heritability, blood pressure polymorphisms, and Mendelian randomization. *Eur Heart J*. 2020;41(35):3314–22. <https://doi.org/10.1093/eurheartj/ehaa238>.
57. Xie Y, Shi H, Han B. Bioinformatic analysis of underlying mechanisms of Kawasaki disease via weighted gene correlation network analysis (WGCNA) and the least absolute shrinkage and selection operator method (LASSO) regression model. *BMC Pediatr*. 2023;23(1):90. <https://doi.org/10.1186/s12887-023-03896-4>.
58. Ou W, et al. Development of a blood proteins-based model for bronchopulmonary dysplasia prediction in premature infants. *BMC Pediatr*. 2023;23(1):304. <https://doi.org/10.1186/s12887-023-04065-3>.
59. Wilde CG, Griffith JE, Marra MN, Snable JL, Scott RW. Purification and characterization of human neutrophil peptide 4, a novel member of the defensin family. *J Biol Chem*. 1989;264(19):11200–3.
60. Szyk A, et al. Crystal structures of human alpha-defensins HNP4, HD5, and HD6. *Protein Sci*. 2006;15(12):2749–60. <https://doi.org/10.1110/ps.062336606>.
61. Wu Z, et al. Human neutrophil alpha-defensin 4 inhibits HIV-1 infection in vitro. *FEBS Lett*. 2005;579(1):162–6. <https://doi.org/10.1016/j.febslet.2004.11.062>.
62. Buturovic L, et al. A 6-mRNA host response classifier in whole blood predicts outcomes in COVID-19 and other acute viral infections. *Sci Rep*. 2022;12(1):889. <https://doi.org/10.1038/s41598-021-04509-9>.
63. Overmyer KA, et al. Large-Scale Multi-omic analysis of COVID-19 severity. *Cell Syst*. 2021;12(1):23–e4027. <https://doi.org/10.1016/j.cels.2020.10.003>.
64. Villanueva E, et al. Netting neutrophils induce endothelial damage, infiltrate tissues, and expose immunostimulatory molecules in systemic lupus erythematosus. *J Immunol*. 2011;187(1):538–52. <https://doi.org/10.4049/jimmunol.100450>.
65. O'Hanlon TP, et al. Gene expression profiles from discordant monozygotic twins suggest that molecular pathways are shared among multiple systemic autoimmune diseases. *Arthritis Res Ther*. 2011;13(2):R69. <https://doi.org/10.1186/ar3330>.
66. Lu X, et al. Peptidoglycan recognition proteins are a new class of human bactericidal proteins. *J Biol Chem*. 2006;281(9):5895–907. <https://doi.org/10.1074/jbc.M511631200>.
67. Yashin DV, et al. Tag7 (PGLYRP1) in complex with Hsp70 induces alternative cytotoxic processes in tumor cells via TNFR1 receptor. *J Biol Chem*. 2015;290(35):21724–31. <https://doi.org/10.1074/jbc.M115.639732>.
68. Yashin DV, Romanova EA, Ivanova OK, Sashchenko LP. The Tag7-Hsp70 cytotoxic complex induces tumor cell necroptosis via permeabilisation of lysosomes and mitochondria. *Biochimie*. 2016;123:32–6. <https://doi.org/10.1016/j.biochi.2016.01.007>.
69. Sharapova TN, et al. Protein PGLYRP1/Tag7 peptides decrease the Proinflammatory response in human blood cells and mouse model of diffuse alveolar damage of lung through blockage of the TREM-1 and TNFR1 receptors. *Int J Mol Sci*. 2021;22(20):11213. <https://doi.org/10.3390/ijms222011213>.
70. Chen Z, Xu J, Sui J, Dai H. Expressions of peptidoglycan recognition protein 1, neuron towards axon guidance Factor-1 and miR-142-3p and their correlations in patients with rheumatoid arthritis. *Int J Gen Med*. 2023;16:3457–64. <https://doi.org/10.2147/ijgm.s418396>.
71. Vökel S, et al. Serum proteomics hint at an early T-cell response and modulation of SARS-CoV-2-related pathogenic pathways in COVID-19-ARDS treated with ruxolitinib. *Front Med (Lausanne)*. 2023;10:1176427. <https://doi.org/10.3389/fmed.2023.1176427>.
72. Steppan CM, et al. The hormone resistin links obesity to diabetes. *Nature*. 2001;409(6818):307–12. <https://doi.org/10.1038/35053000>.
73. Nozue H, et al. Serum resistin concentrations in children with Kawasaki disease. *Inflamm Res*. 2010;59(11):915–20. <https://doi.org/10.1007/s00011-010-0202-8>.
74. Bo S, et al. Relationships between human serum resistin, inflammatory markers and insulin resistance. *Int J Obes (Lond)*. 2005;29(11):1315–20. <https://doi.org/10.1038/sj.ijo.0803037>.
75. Shetty GK, Economides PA, Horton ES, Mantzoros CS, Veves A. Circulating adiponectin and resistin levels in relation to metabolic factors, inflammatory markers, and vascular reactivity in diabetic patients and subjects at risk for diabetes. *Diabetes Care*. 2004;27(10):2450–7. <https://doi.org/10.2337/diacare.27.10.2450>.
76. Hemmat N, et al. Neutrophils, crucial, or harmful immune cells involved in coronavirus infection: A bioinformatics study. *Front Genet*. 2020;11:641. <https://doi.org/10.3389/fgene.2020.00641>.
77. Shaw AC, Goldstein DR, Montgomery RR. Age-dependent dysregulation of innate immunity. *Nat Rev Immunol*. 2013;13(12):875–87. <https://doi.org/10.1038/nri3547>.
78. Pagliaro P. Is macrophages heterogeneity important in determining COVID-19 lethality? *Med Hypotheses*. 2020;143:110073. <https://doi.org/10.1016/j.mehy.2020.110073>.
79. Furukawa S, et al. Serum soluble CD4 and CD8 levels in Kawasaki disease. *Clin Exp Immunol*. 1991;86(1):134–9. <https://doi.org/10.1111/j.1365-2249.1991.tb05785.x>.
80. Naoe S, Takahashi K, Masuda H, Tanaka N. Kawasaki disease. With particular emphasis on arterial lesions. *Acta Pathol Jpn*. 1991;41(11):785–97. <https://doi.org/10.1111/j.1440-1827.1991.tb01620.x>.
81. Furukawa S, Matsubara T, Yabuta K. Mononuclear cell subsets and coronary artery lesions in Kawasaki disease. *Arch Dis Child*. 1992;67(6):706–8. <https://doi.org/10.1136/adc.67.6.706>.
82. Ding Y, et al. Profiles of responses of immunological factors to different subtypes of Kawasaki disease. *BMC Musculoskelet Disord*. 2015;16:315. <https://doi.org/10.1186/s12891-015-0744-6>.
83. Kobayashi M, et al. Histologic and immunohistochemical evaluation of infiltrating inflammatory cells in Kawasaki disease arteritis lesions. *Appl Immunohistochem Mol Morphol*. 2021;29(1):62–7. <https://doi.org/10.1097/PA.1000000000000860>.
84. Wang Z, et al. Single-cell RNA sequencing of peripheral blood mononuclear cells from acute Kawasaki disease patients. *Nat Commun*. 2021;12(1):5444. <https://doi.org/10.1038/s41467-021-25771-5>.
85. Wright VJ, et al. Diagnosis of Kawasaki disease using a minimal Whole-Blood gene expression signature. *JAMA Pediatr*. 2018;172(10):e182293. <https://doi.org/10.1001/jamapediatrics.2018.2293>.
86. Kuniyoshi Y, et al. Comparison of machine learning models for prediction of initial intravenous Immunoglobulin resistance in children with Kawasaki

disease. *Front Pediatr.* 2020;8:570834. <https://doi.org/10.3389/fped.2020.570834>.

### **Publisher's note**

Springer Nature remains neutral with regard to jurisdictional claims in published maps and institutional affiliations.